Smart Structures and Systems, *Vol. 27, No. 4 (2021) 559-569*
DOI: https://doi.org/10.12989/sss.2021.27.4.559

Direct tensile strength measurement of granite by the universal tensile testing machine

Hadi Haeri [1], Vahab Sarfarazi*[2], Mohammad Fdatehi Marji [3a], Mohammad Davood Yavari [4] and Amin Zahedi-Khameneh [5]

[1] *State Key Laboratory for Deep GeoMechanics and Underground Engineering, Beijing, 100083, China*
[2] *Department of Mining Engineering, Hamedan University of Technology, Hamedan, Iran*
[3] *Head of Mine Exploitation Engineering Department, Faculty of Mining and Metallurgy, Institution of Engineering, Yazd University, Yazd, Iran*
[4] *Department of mining Engineering, Bafgh Branch, Islamic Azad University, Bafgh, Iran*
[5] *Department of Civil Engineering, Malard Branch, Islamic Azad University, Malard, Iran*

(*Received January 1, 2020, Revised November 16, 2020, Accepted December 14, 2020*)

Abstract. The direct tensile strength of a typical hard rock like granite is measured by a novel apparatus known as compression-to-tensile load transfer (CTLT) device. The rock specimen is prepared in form of a slab containing a central hole and placed in the universal testing machine where the direct tensile stress can be applied to this specimen by implementing a special type of load transferring device which converts the applied compressive load to that of the tensile during the test. In the present work, some typical hard rock specimens of granite are specially prepared and tested in the laboratory to measure their direct tensile strengths. Then, a new load converting device implemented in the universal tensile testing machine is used to cause the rock specimen to be subjected to a direct tensile loading during the test. The compressive load was applied to the transferring device at the rate of 0.02 MPa/s. Numerical modeling of the tested specimens were accomplished using the discrete element method (DEM) and the higher order displacement discontinuity method (HODDM). The tensile failure of granite rock mainly occurs along the horizontal axis. The experimental results were in a good accordance with DEM results and HODDM outputs.

Keywords: failure stress measurement; universal testing machine; granite specimens; numerical simulation

1. Introduction

In the modern rock mechanics literature, the direct measurement of rocks' tensile strengths is of paramount importance in most of the surface and underground rock structures. The indirect tensile strength tests especially the Brazilian tensile tests are widely used in most rock engineering projects because of their simplicity and easy preparation of laboratory rock specimens (Bieniawski and Hawkes 1978, Zhang 2002, Martin 2014, Sardemir 2016, Sarfarazi *et al*. 2017, Liu *et al*. 2018, Shang *et al*. 2018, Liao *et al*. 2019, Aliabadian *et al*. 2019, Albegmprli *et al*. 2019). However, the values of the indirect tensile strengths obtained from the Brazilian tests are overestimated (about 26 percent) which may be doubtful in many modern rock applications (Gorski *et al*. 2007). A plenty of theoretical and experimental works were performed to accurately measure or calculate the tensile strength of rocks and concretes (Zhou 1988, Wang *et al*. 2004, Ghaffar *et al*. 2005, Erarslan and Williams 2012, Wei and Chau 2013, Ramadoss and Nagamani 2013, Kim and Taha 2014, Pan *et al*. 2014, Silva *et al*. 2015, Sarfarazi *et al*. 2015, Abrishambaf *et al*. 2015, Sardemir 2016, Shuraim *et al*. 2016, Hu *et al*. 2016, Li *et al*. 2016, Zhang *et al*. 2016, Alhussainy *et al*. 2016, Mosaberpanah and Eren 2016, Akbas 2016, Yaylac 2016, Sarfarazi *et al*. 2017, Omar *et al*. 2018, Tran *et al*. 2019, Forti *et al*. 2019, Maruvanchery and Kim 2019, Sun *et al*. 2019). In the case of concretes, the tensile strength can be measured by preparing some special specimens of different dimensions and shapes and carry out the experimental tests such as the direct pull tests carried out on rock like specimens having dumb-bell shapes (Xie and Liu 1989, ASTM D2936-08 2008, Zheng *et al*. 2001). Other tensile strength measuring tests such as (indirect) tests on discs (cylinders), rings or cubes, the flexural tests on beams (three points and four points bending tests) and double punch tests were also extensively used to measure the tensile strength of rocks and concretes (Hannant 1972, Chen and Trumbauer 1972).

Some direct tension tests were carried out by Swaddiwudhipong *et al*. (2003) to determine the concretes' tensile strength based on the strain capacity of concrete specimens provided from different cements. Compared with the indirect testing approach, the direct measuring methods require a significant amount of sample preparations and careful measuring apparatus. Some other drawbacks of the direct tension measuring tests are: the load eccentricity and failure surface rotation, non-symmetric specimens and asymmetric deformations in the damaged and failed zones (Zhou 1988). All these factors may result on the moment in the specimens and around the failed zones which definitely

*Corresponding author, Associate Professor,
E-mail: vahab.sarfarazi@gmail.com
[a] Associate Professor

ISSN: 1738-1584 (Print), 1738-1991 (Online)

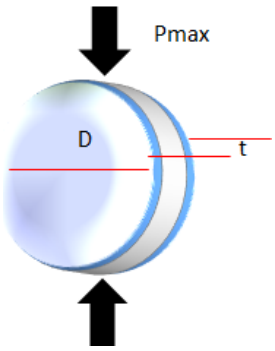

Fig. 1 The schematic view of a Brazilian indirect tensile strength measuring test

affect the tensile strength of the brittle materials such as concretes and rocks. Kim and Taha (2014) conducted some direct tensile tests on the concrete cylindrical specimens. They tried to establish a uniform stress distribution along the failure plane of the concrete specimens while performing the direct tensile testing. They assessed and confirmed that the failure (cracking) zone in direct tensile testing can depend on the distribution of specimens' unit weight. The Brazilian tensile strength test on cylindrical specimens (ASTM D33967-16 31) as shown schematically in Fig. 1. may be considered as the most reliable indirect testing method which reasonably gives a lower variation coefficient. Considering a cylindrical specimen with diameter **D**, thickness ***t*** which fails under a loading P_{max} during a Brazilian test. The tensile strength of this specimen can be measured by the following formula

$$\sigma_t = \frac{2P_{max}}{\pi D t} \quad (1)$$

The relation of indirect tensile strength of a high strength concrete to that of its uniaxial compressive strength has been studied by Zain *et al*. (2002). Most of the existing tensile strength tests may have limitations due to for example the linear elastic behavior assumptions for the rocks and rock-like materials. On the other hand, during the test a uniform tensile stress may not be achieved on the splitting failure. This may cause that this surface deviate from being uni-axial and the induced tensile stress gradually increases toward the specimen's center (Khan 2012). A rough and approximated value of the concrete and rock tensile strength may be achieved due to the above mentioned drawbacks of the indirect tensile testing methods. The rupture modulus of rocks and concretes may also be measured by evaluating its resistance to indirect tensile cracking using 3- and/or 4-point bending tests. These tests also over-estimate the real value of the rock and concrete tensile strengths (Gorski *et al*. 2007).

Therefore, it seems reasonable to develop a more reliable tensile testing apparatus to get a more precise value of rocks' tensile strength in the laboratory. In the present study, it is tried to develop a new direct tensile testing apparatus to overcome the limitations and draw backs of the indirect tests. This specially designed device is a compression-to-tensile load transfer (CTLT) which uses some specific types of rocks or concretes specimens. The present paper also explains the preparation of specimens for this specially designed apparatus. The specimens may be prepared in various dimensions but in this paper the specimen's dimension are taken as 19 cm ×15 cm × 6 cm. To transfer the compressive load to that of the tensile one, a central hole having a diameter of 7.5 cm and a thickness of 6 cm, is provided at the center of each rock samples by dry drilling. For all specimens, the ratio of central holes' diameter to the width of the specimen is taken as 0.5.

The experimental works needed for performing the tests by this apparatus in a rock mechanics laboratory are explained and the design steps and assembly of the CTLT device are presented. Then some numerical simulation of the experimental work is carried out to further demonstrate the accuracy and effectiveness of the proposed failure stress measuring device.

2. Compressive-to-tensile load transferring (CTLT) apparatus

It is usually difficult to measure the direct tensile strength of rocks and concretes in the ordinary laboratory testing apparatuses. Therefore, a new compressive-to-tensile load transferring (CTLT) apparatus is specially designed for directly measuring the tensile strength of rocks while loaded under normal compression. The specimens are specially prepared to have a central hole in the middle so that provide the means to transfer the compressive loading to that of the tensile as required in CTLT while is placing in the universal testing machine. Figs. 2(a) to (d) illustrate the various parts and their dimensions for a CTLT device, respectively. Fig. 2(a) show the "U" shape segment of the device (Part No. I) which built from stainless steel and consists of two parts i.e., "L" and "1" shape sub-segments. The second part (Part No. II) is shown in Fig. 2(b) which is undividable and have "II" shape. The third part (Part No. III) is shown in Fig. 3(b) which consists of two semi-cylindrical stainless steels sub-segments with dimensions of 75 mm × 10 mm × 60 mm. the last part (Part No. IV) of the device is shown in Fig. 2(d) and consists of two blades with dimensions of 20 mm × 10 mm × 190 mm.

Figs. 3(a) to (f), show the set up procedure of CTLT device, respectively, to perform a useful direct tensile strength measuring process for brittle geo-materials such as concretes and rocks. This set up procedure is divided into six different stages as: (i) the Part No. III (as shown in Fig. 3(a)) are inserted into the specimens' central hole; (ii) The "L" shape segment of Part No. I is situated on the specimens' left side (see Fig. 3(b)); (iii) the first blade of Part No. 4 inserted on the upper part of the hole to be in contact with the Part No. III (cylindrical steel form above and also its lower surface is contact with the "L" shape segment of Part No. I (as illustrated in Fig. 3(c)); (iv) the Part No. II is placed on the specimens' right side as shown in Fig. 3(c); (v) the second blade of Part No. IV is situated in the lower surface of the central hole to be in contact with the cylindrical steel. As shown in Fig. 3(d), the upper part of the second blade is in contact with the "I" shape segment of Part No. II; and finally, (vi) the "I" shape segment of Part

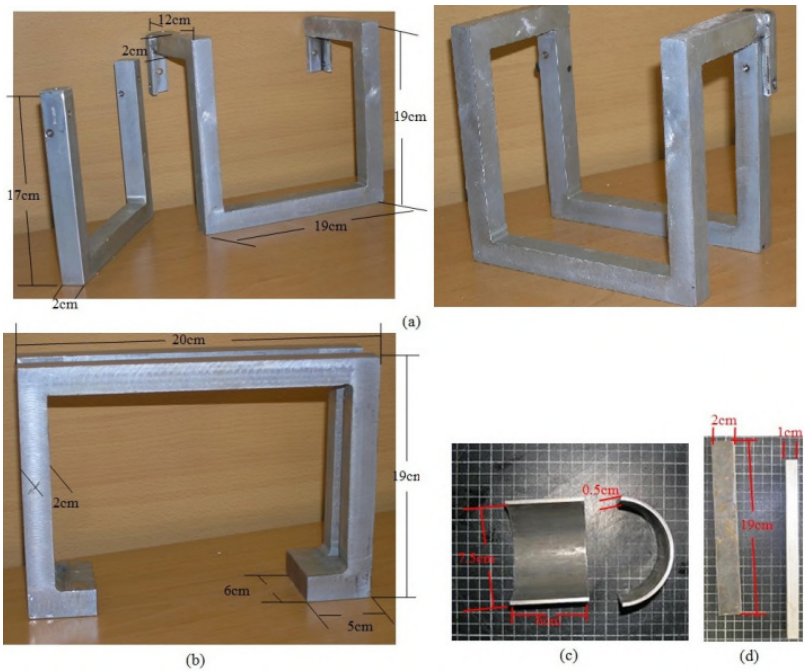

Fig. 2 Different parts of CTLT device

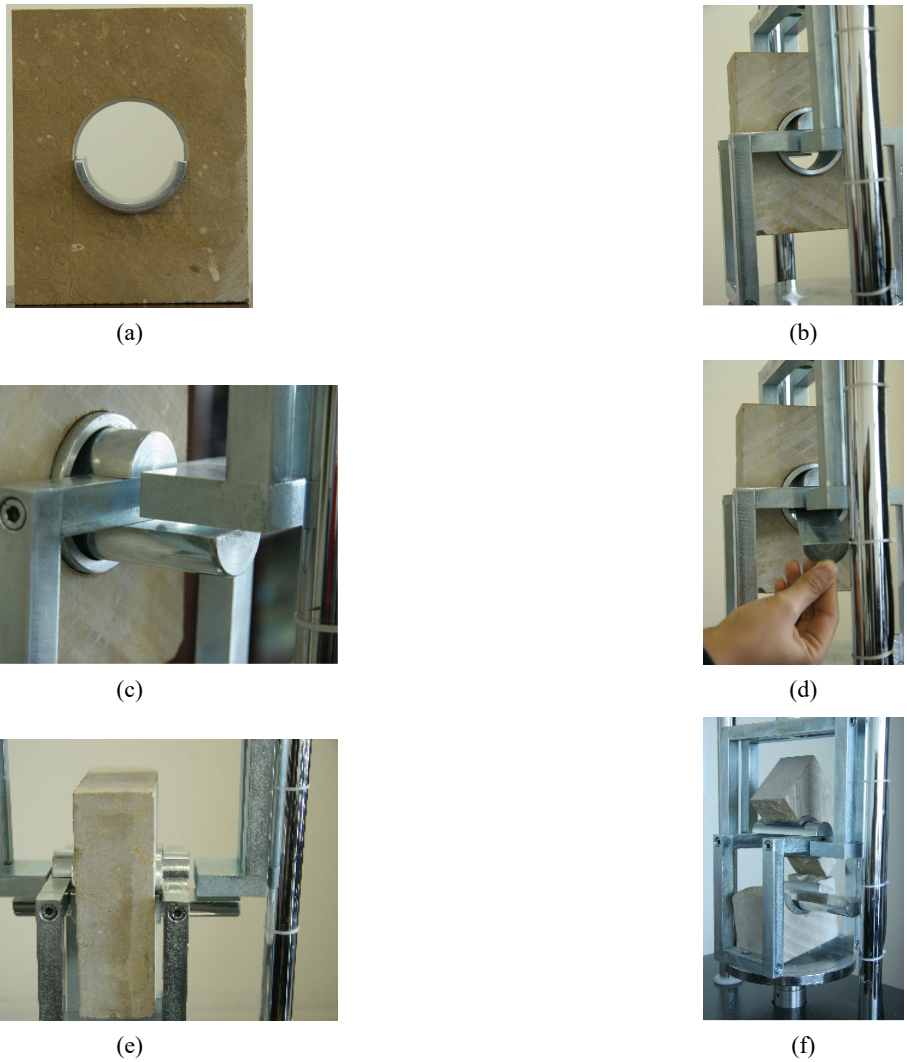

Fig. 3 The set up procedure of CTLT device

Fig. 4 A central hole of diameter of 7.5 cm and thikness of 6 cm is drilled at the specimens' center

No. II is screwed to the "L" shape segment of Part No. I. As shown in Fig. 3(e), the upper section of the specimen is in contact with the lower cylindrical steel and the lower section is in contact with the upper cylindrical steel. In this procedure, the completed set up is placed in the uniaxial compression loading frame. Then when the specimens' upper part is compressed its lower part moves down and when the specimens' lower part is compressed its upper part moves up and as a whole a direct tensile loading is bear by the specimen (Fig. 3(f)).

2.1 Rock Specimen's preparation for CTLT device

Some granitic rock samples with a mass density of 2.57 gr/cm3 were provided to prepare the required experimental specimens for the CTLT device in the laboratory. The prepared specimen's dimensions were 19 cm × 15 cm × 6 cm, with a central hole of 7.5 cm in diameter and 6 cm in height. The dry drilling technique is used to remove a central rock core from the rock specimens' center (Fig. 4). In this case, the ratio of central hole diameter to that of the sample's width is 0.5. This type of rock specimen can be easily prepared in any standard rock mechanics laboratory.

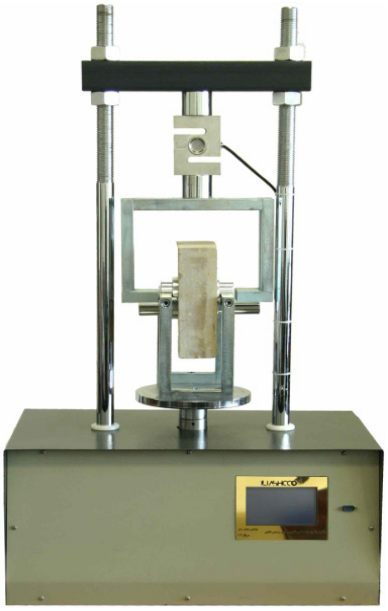

Fig. 5 The Universal Tensile Testing Machine (UTTM)

A complete direct tensile testing arrangement of CTLT is illustrated in Fig. 5 (The Universal Tensile Testing Machine or UTTM). The UTTM can use a CTLT containing a rock specimen which is installed in a uniaxial compression

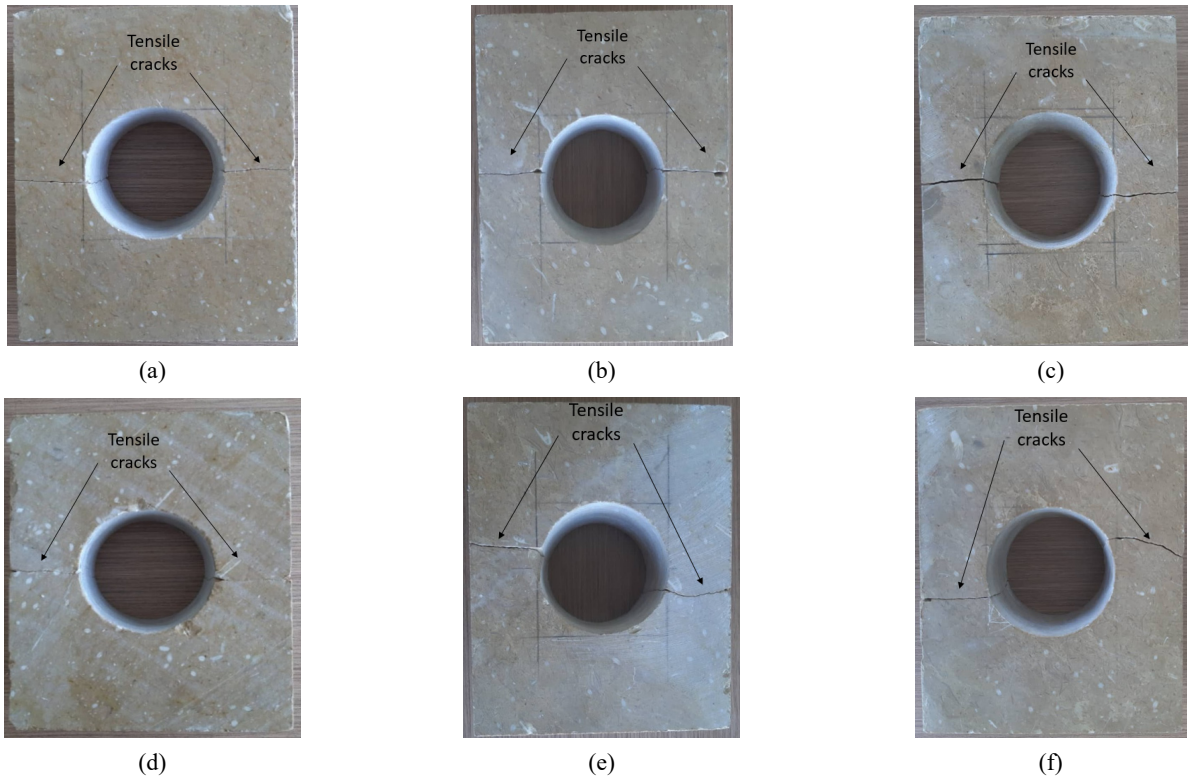

Fig. 6 The direct tensile failure pattern in CTLT specimens

loading frame. This loading frame is specially designed to apply a uniaxial compressive load to the CTLT end plates via a 5-tons gearbox load cell. The applied load increments can be measured by an electronic load cell. The effect of loading rate on the final results is minimized by applying a constant loading rate (i.e., 0.02 MPa/s) during the testing operation. Denneman (Denneman *et al*. 2011) suggested this loading rate for tensile strength measurement by rock splitting procedures.

2.2 Direct tensile strength test by CTLT

The main features of a UTTM can be summarized as: (i) Powered by a single-phase electricity and have a rigid frame with a loading capacity of 5 tons; (ii) recording the test data in Excel, plotting displacement-force and stress-strain curves and simultaneously registering the values of stress and corresponding strain; (iii) portable with touch screen display and includes engine and gearbox for applying force (by using aluminum loading bars) at a constant rate of 1 kg/s without a slippery motion; (iv) measuring the uniaxial compressive and tensile strengths and fracture toughnesses of concretes, asphalts, rocks, mortars and ceramics. It may be noted that although the uniaxial compressive strength of hard rocks cannot be measured by this apparatus but the compressive strength of soft to medium rocks and rock like materials can be successfully measured.

In this work, a total number of 12 granitic rock specimens are prepared in a rock mechanics laboratory. The direct rock's tensile strength is measured by preparing six special pre-holed rectangular specimens to be tested using the CTLT device in UTTM (Figs. 6(a) to (f)). The other six specimens are subjected to splitting tests i.e., the conventional indirect (Brazilian) tensile strength tests as shown in Figs. 7(a) to (f).

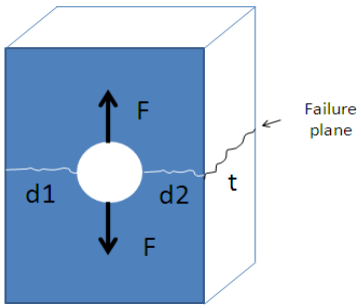

Fig. 7 The parameters used for the calculation of rock's direct tensile strength

Table 1 The failure stress of typical granitic rock specimens

Experimental failure stress (MPa)	
6.5	
6.4	
6.6	
6.5	
6.3	
Average	6.46

As shown in Figs. 6(a) to (f), it is easily observed that all these specimens are failed (cracked) through a horizontal line starting from the center hole when the specimen is subjected to a vertically applied compression by the loading frame. This is a tensile failure or a splitting tensile failure which is produced by the two hollow semi-cylindrical steels (forming a steel ring around the central hole of the specimen).

2.3 Measuring the failure stress of rocks by UTTM

The failure stress of rock (σ_t) can then be calculated through the following simple formula

$$\boldsymbol{\sigma_t = \frac{F}{(d1 + d2) \times t}} \quad (2)$$

where σ_t is the failure stress (in kg/cm^2), ***F*** is the force at failure (in kg), ***d1*** and ***d2*** are the width of intact sample on the both sides of the central hole (in cm) and ***t*** is thickness of the specimen (in cm) (Fig. 7).

The failure stress were presented in Table 1. The average failure stress value measured by using CTLT device is about 6.5 MPa.

Further verification of the failure stress obtained by using the CTLT device in UTTM can be made by simulating the rock testing specimens through some numerical techniques such as the discrete element method (DEM) and indirect boundary element method (BEM). In the present work, the particle flow code in two-dimensions (PFC2D) based on DEM is used to check the experimental failure stress values for a typical granite. A semi-analytical two-dimensional indirect boundary element method (the higher order displacement discontinuity method) is also used in this study to further verify the experimental and numerical results.

3. Discrete element analyses of the rock specimens used in tensile strength tests

In the discrete element analyses of the rock samples by the two dimensional particle flow code (PFC2D) the material sample is simulated as an assembly of the circular discs bonded at the contact points which are confined by the planar side walls. In this modelling technique, a competent laboratory rock sample can be modelled as an assembly of bonded particles which are kept in contacts with each other by the internal contact forces. There are basically two types of bonding models known as the contact and the parallel bonded models which are usually used in the discrete analyses of geo-materials such as rocks and concretes. In a contact bonded model, the physical behavior of the material is approximated by a vanishingly thin layer of cement-like substance (matrix) lying in between the two-bonded particles and joining them. On the other hand, in a parallel bonded model each bond has a radius at its contacts with the neighboring particles. Thus, a contact bonded model is the same as a parallel bonded model of zero radius.

Table 2 Micro properties used to numerically simulate the intact rock specimens

Parameter	Value	Parameter	Value
Type of particle	disc	Stiffness ratio	2
Density (kg/m^3)	3600	Particle friction coefficient	0.5
Minimum radius (mm)	0.27	Contact bond normal strength, mean (MPa)	45
Size ratio	1.56	Contact bond normal strength, SD (MPa)	2
Porosity ratio	0.08	Contact bond shear strength, mean (MPa)	45
Damping coefficient	0.7	Contact bond shear strength, SD (MPa)	2
Contact young modulus (GPa)	55	Radius multiplier	1.2

For a contact model, there is no shear and/or normal stiffness with no resistance to the bending moment and only forces are acting at the contact points in between the particles. As stated by Cundall and Strack (1979) and Itasca (2003), the tensile and shear strengths are assigned to exist at the contact bonded model which allow the material resistance against tension and shear until these forces exceed the tensile and shear strengths of the modelled geo-materials. Some special types of subroutines are provided by Cundall and Strack (1979) to generate the contact and parallel bonded particle models. They defined the following micro-mechanical and geometrical parameters for simulating the macro-mechanical parameters determined in the laboratory: (i) contact modulus for the ball-to-ball contacts of particles; (ii) the balls' coefficient of friction; (iii) the contact normal and shear bond strengths; (iv) the ratio of standard deviation to that of the mean normal and shear bonding strengths; (v) the stiffness ratio Kn/Ks (Kn is normal stiffness of spring between two discs and Ks is shear stiffness of spring between two discs); (vi) the radius multiplier (Radius multiplier is a coefficient that multiple in disc radii to reach a desired isotropic stress: the standard value for isotropic stress in bonded particle model was 1 MPa. This value should be defined for numerical model to reach the best contacts between the discs.), bond modulus and stiffness ratio of the parallel bonds.

In this research, the parallel bonded model, plane strain condition of linear elasticity and a unit thickness are assumed for the numerical simulation of the rock samples.

3.1 Numerical simulation of Brazilian tensile strength test

A standard calibration of the numerical modelling technique is accomplished by simulating the Brazilian tensile strength testing of rock samples in PFC2D. The standard calibrating procedure proposed by Potyondy and Cundall (2004) is adopted using the micro-properties of the model as listed in Table 2. The micro-parameters were proposed by authors. The simulated specimen was made of 5615 particles assuming a Brazilian disc of 54 mm. in diameter. Then, the loading walls of the specimens were moved toward each other at a low constant speed of 0.016 mm/s to establish a Quasi-static equilibrium condition for the rock specimen. It should be noted that the model porosity was fixed at 0.08 which was suitable for the calibrated model (although this porosity ratio may be different from that of the actual rock sample. This value affect the disc numbers and disc numbers affect the failure mechanism of model).

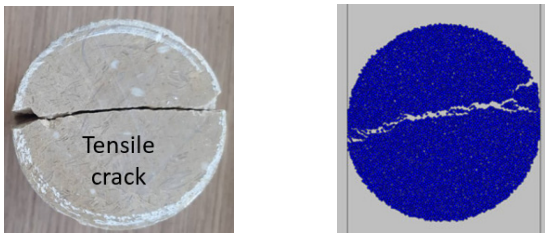

(a) (b)

Fig. 8 (a) Experimental Brazilian tensile strength test; and (b) numerically simulated Brazilian tensile strength test

The experimental Brazilian testing specimen is shown in Figs. 8(a) while Fig. 8(b) shows the corresponding numerically simulated specimen. The formula for calculation of tensile strength of numerical models is in ASTM D3967-16 (2016). Comparing the numerical and experimental tensile strength values show that these results match each other (i.e., the experimental and numerical values of the tensile strength for the typical granitic rock sample are 8.5 and 8.7 MPa, respectively). Figs. 8(a) and (b) shows the experimental Brazilian test and numerical Brazilian test, respectively. The results show well matching between experimental test and numerical simulation. Therefore, the numerical method using these micro-parameters is calibrated and can be effectively used further for the solution of the proposed problem cited in this research work.

3.2 Numerical simulation of CTLT testing specimens using particle flow code (PFC)

As shown in Fig. 9, a box model representing the rock sample of 75 mm × 100 mm is created in PFC2D using a total number of 11,179 circular discs with a minimum radius of 0.27 mm. Then, a hole of various diameters, B (B = 10, 15, 20, 25 and 30 mm) is placed in the central part of the box model to simulate the CTLT specimens used for determining the direct tensile strength of rock using the UTTM. After preparing the numerical model, two semi-circular load-bearing walls (wall No. 1 and wall No. 2 in Fig. 9) are modeled to be in contact with the central hole (Fig. 9). The upper and lower parts of the specimen's walls are pulled up (in the positive Y-direction) to apply tensile

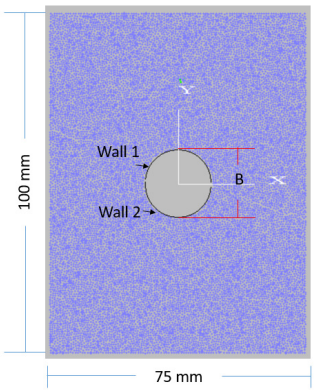

Fig. 9 Specification for the numerical modelling of CTLT testing specimens with a hole diameter

loading to the modelled specimen. During the testing process, the tensile is registered considering the reaction forces on one of the walls (wall No. 1 in this study).

3.3 Tensile failure mechanism

The direct tensile failure mechanism of rock specimens is studied experimentally and numerically in this research. Then a comparison is performed between these two sets of results to visualize the similarity of them and verifying the effectiveness and accuracy of the proposed direct method.

3.3.1 Numerical models vs experimental testing results

Figs. 10(a) to (e) illustrate the process of crack propagation in CTLT specimens during the test performance.

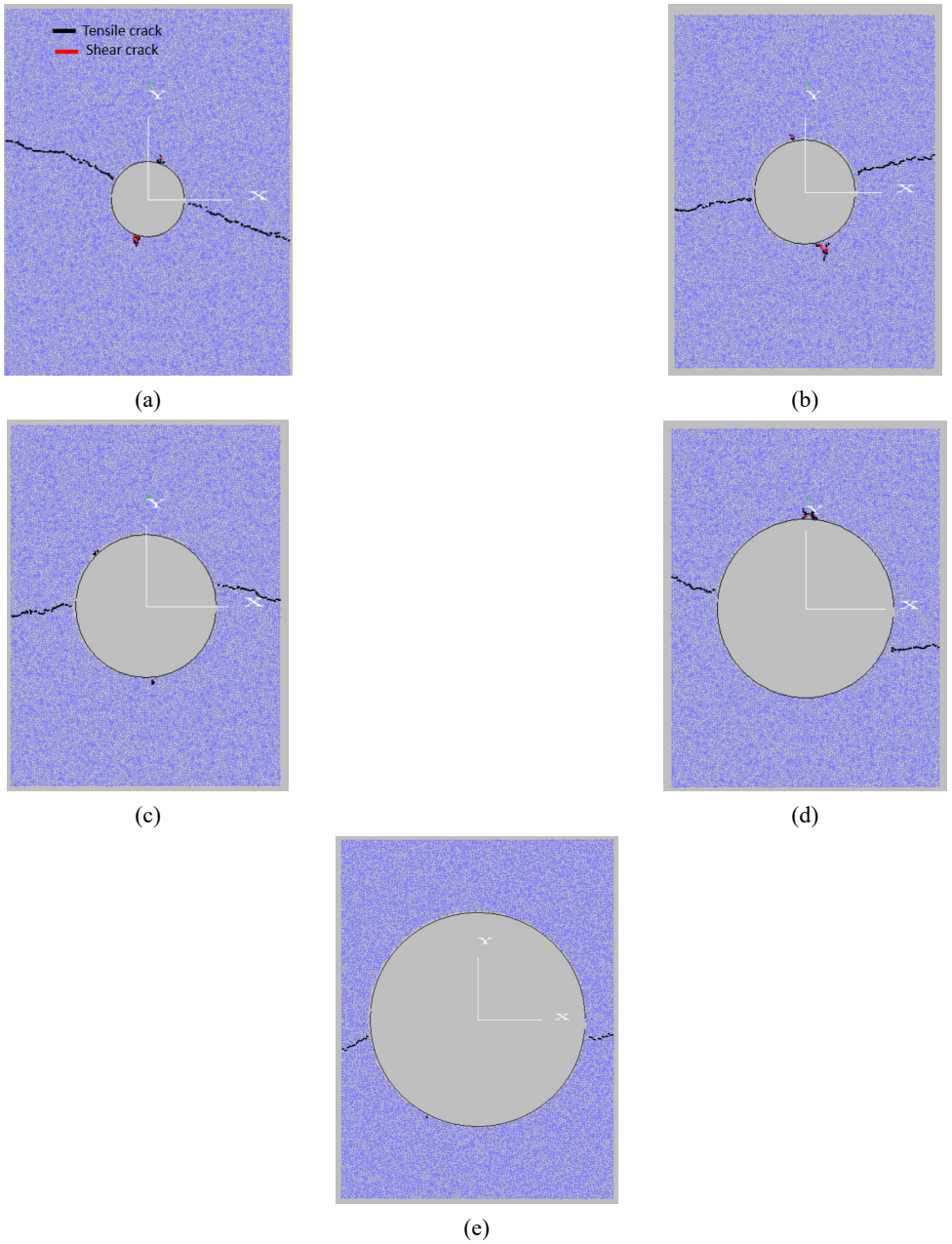

Fig. 10 Failure pattern of the numerically modeled CTLT specimens each containing a central hole of diameter: (a) 10 mm; (b) 15 mm; (c) 20 mm; (d) 25 mm; and (e) 30 mm

Table 3 The values of failure stress obtained by numerical simulation

The internal hole diameter (mm)	Numerical direct failure stress (MPa)
10	7.1
15	7
20	7
25	7.04
30	6.8

In these figures, the black and red lines demonstrate the tensile (primary) and shear (secondary) cracks, respectively. The cracked models illustrate that during the failure process a horizontal line crack is propagating through the center of the hole. Therefore, the crack starts to propagate from the ends of the horizontal diameter and lead to final rupture. The same scenario can be visualized from the experimental tests already shown in Fig. 6.

3.3.2 Failure stress gained from the numerically simulated CTLT specimens

In this section the numerically approximated results of direct failure stress and indirect tensile strengths are tabulated in Table 4. The failure stresses were decreased by increasing the hole diameter. In fact, by increasing the hole diameter, two rock segments at both sides of hole will be narrow and the plane strain condition changes to plane stress condition. This leads to decreasing the failure stress value by increasing the hole diameter.

It is visualized that the direct failure stress values presented in Table 3 are very close to those already given in Table 1 (the laboratory measured values).

4. Displacement discontinuity analyses of the pre-holed rock specimens used by CTLT device

The quadratic or cubic (higher order) variations of the displacement discontinuity (DD) along line cracks in a linear elastic material (Marji 1997, Hosseini_Nasab and Fatehi Marji 2007, Marji 2013). This kind of the indirect boundary element method as proposed by Crouch and Starfield, 1982 can be used to obtain the displacements, stresses and stress intensity factors in the cracked rock samples (Marji *et al*. 2007, Haeri *et al*. 2015). In the present research, a higher order two-dimensional displacement discontinuity code (HODDM-2D) is used to numerically model the pre-holed rectangular specimen of CTLT device. This higher order DD method is based on the cubic DD variations with four sub-elements of equal lengths along each batch element as proposed by Marji *et al*. (2007).

The displacement and stress fields and stress intensity factors near a crack tip can be evaluated based on the formulations given in the literature e.g., in reference (Marji *et al*. 2007). The accuracy of the displacement discontinuities can be further increased by using some special crack tip elements to model the singularities of the crack tips. The detailed formulations are not given here and the reader is referred to the reference (Marji *et al*. 2007).

However, in the early 1950's, Irwin, introduced the Mode I (opening Mode) and Mode II (sliding Mode) stress intensity factors (SIFs) based on the linear elastic fracture mechanics (LEFM) principles to study the crack problems in solid mechanics (Whittaker *et al*. 1992, Sanford 2003). These SIFs are denoted by K_I and K_{II}, and usually expressed in MPa $m^{1/2}$. The normal and shear displacement discontinuities obtained near the crack tips can be used to estimate the values of by K_I and K_{II} (Shu and Crouch 1995, Hosseini_Nasab and Fatehi Marji 2007, Marji *et al*. 2007). In this study, based on the linear elastic fracture mechanics (LEFM) principles, the mixed mode in-plane fracture criterion such as σ-criterion is used to estimate the maximum tensile stress at the failure (Whittaker *et al*. 1992, Hosseini_Nasab and Fatehi Marji 2007).

4.1 Displacement Discontinuity analysis of a rectangular specimen containing a central circular hole

In this research, the problem of a rectangular specimen with a hole at its centre is numerically modelled by a higher order displacement discontinuity method in two dimensions (HODDM-2D). A small initial crack was modelled at the points with maximum stress concentration**.** As explained briefly in the previous section, the third order displacement discontinuity elements with four sub-elements of equal lengths used to predict the fracture propagating process of the CTLT specimens due to direct tensile loading and estimating the direct tensile strength numerically.

As shown in Fig. 11, this method uses two sub-elements on each side of a batch element's centre (i.e., four collocation displacement discontinuity points is considered for each boundary element). This indirect boundary element method is modified to model the crack problems in finite, infinite, and semi-infinite plane elasticity. The accuracy of the original constant element displacement discontinuity method (DDM) developed by Crouch (1976) is highly increased by using this proposed approach (Marji *et al*. 2007).

In this study, the pre-holed rectangular rock specimens are numerically modelled by the HODDM considering 20 third order (cubic) DD elements along the outer boundary of the specimen and also the central hole's boundary is simulated by taking 10 cubic DD elements as shown in

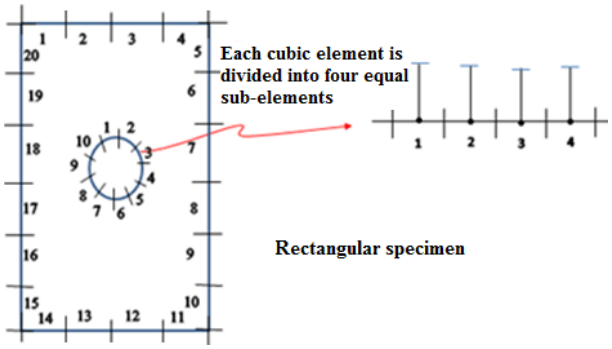

Fig. 11 Boundary discretization for a pre-holed rectangular specimen

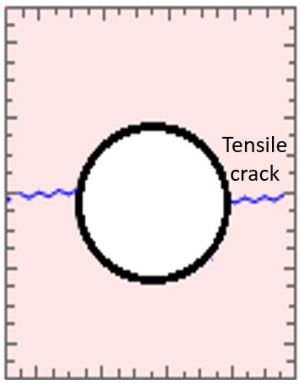

Fig. 12 Displacement discontinuity modelling of the tensile crack propagation paths for a pre-holed rectangular specimen

Fig. 13 (the dimensions are the same as those used experimentally in the direct tensile test instrument).

Based on the LEFM concepts, the tensile cracks propagation paths and directions are predicted by using the iterative method and calculating the crack propagation angle θ at each crack tip in different steps.

The numerical crack propagation process is illustrated in Fig. 12 The crack growth paths in numerical models show that two tensile cracks begin from both sides of the hole and propagate horizontally till meeting the boundaries of the rectangular model in the middle part. An appropriate mixed mode in-plane fracture criterion such as σ-criterion (used in this study) has been chosen to investigate the cracks propagation path and their directions within a modelled pre-holed rectangular rock specimen under compression or tensile loading conditions. For this purpose, two cracks of small length are considered on the either side of the hole. These small cracks are expected to be initiated and propagated in a direction perpendicular to that of the applied tensile load. Therefore, as shown in Fig. 12, two small edge cracks are taken on either side of the hole. Considering small tensile cracks of length b, a standard iterative approach is adopted in this numerical modelling technique to estimate the crack propagation paths and directions by incrementally extending the crack tip with an increment of length Δb = 0.1b, in the predicted direction given by the σ-criterion (Marji *et al*. 2007).

The failure stress results estimated by the higher order DD method are compared with the corresponding values experimentally measured in the laboratory by UTTM in Table 4. This table illustrate that the differences between two tests is nearly close to 9%.

As a whole, the PFC2D simulation and HODDM simulation both show that there is a good accordance between the numerical modelling and experimental results for obtaining the failure pattern of rocks.

Table 4 Values of failure stress of rectangular specimens predicted by the higher order DD method and experimentally measured by laboratory test

DDM failure stress (MPa)	Experimentally measured failure stress (MPa)
7.1	6.5

5. Conclusions

In many engineering structures, the strength criteria for intact rock and rock like materials are of essential for a safe and reliable deign, durability and performance. These strength criteria have been mainly derived from tests in the compressive stress region due to the higher strength of rocks under compression and some technical difficulties that may exist in performing and designing the direct tensile strength tests. Therefore, a very few works have been published for the direct tensile tests on rock ad rock like material so that no suitable criteria are available for addressing this issue at the current stage. Thus, the direct tensile strength determination of rocks and rock like materials is one of the major tasks in geo-mechanics. In the present research, a portable universal tensile testing machine (UTTM) is introduced and used to accurately measure the tensile strength of rocks and rock like materials. However, it should be noted that the proposed UTTM is economical and simple which its assemblage is relatively easy. It is designed and fabricated to accurately measure the tensile strengths of rocks subjecting to direct tensile loading. In the study, UTTM was used for direct tensile testing of a typical granite specimen with dimension of 19 × 15 × 6 cm and having a central hole with the ratio of central hole diameter to that of the specimen's width, 0.5. A compression-to-tensile load transferring (CTLT) device containing the pre-holed rectangular specimen is implemented in the UTTM for performing the direct tensile strength test. Under the CTLT test, the rock specimen cracked along a horizontal line starting from the central hole boundaries. Two horizontal tensile fracture propagating from the central hole to the boundary of the specimen cause the final rapturing of the rock sample. The measured value of direct tensile strength of the granitic rock was about 6.5 MPa using UTTM.

The two relatively versatile numerical methods in geo-mechanics i.e., the indirect boundary element method (BEM) and the discrete element method (DEM) have also been used to numerically simulate the pre-holed rectangular rock specimens for measuring the direct tensile strength of rocks. Both the DEM and BEM estimated the direct tensile strength of this granitic rock specimen as about 7 MPa which is very close to its experimental values obtained by using UTTM in the laboratory. However, as it was expected, the direct tensile strength values experimentally obtained from the CTLT device of UTTM were about 32% lower than those measured from the Brazilian (indirect) testing method. Each CTLT testing specimen can be prepared within 30 min. Finally, it is concluded that both PFC2D and higher order DDM simulations of the direct tensile strength measuring specimen show that there is good accordance between the numerical models and experimental results of rock's direct tensile strength.

References

Abrishambaf, A., Barros, J.A. and Cunha, V.M. (2015), "Tensile stress–crack width law for steel fibre reinforced self-compacting concrete obtained from indirect (splitting) tensile tests", *Cement Concrete Compos*., **57**, 153-165. https://doi.org/10.1016/j.cemconcomp.2014.12.010

Akbas, S. (2016), "Analytical solutions for static bending of edge cracked micro beams", *Struct. Eng. Mech., Int. J.*, **59**(3), 66-78. https://doi.org/10.12989/sem.2016.59.3.579

Albegmprli, H.M., Gülşan, M.E. and Cevik, A. (2019), "Comprehensive experimental investigation on mechanical behavior for types of reinforced concrete Haunched beam", *Adv. Concrete Constr., Int. J.*, **7**(1), 39-50. https://doi.org/10.12989/acc.2019.7.1.039

Alhussainy, F., Hasan, H.A., Rogic, S., Sheikh, M.N. and Hadi, M.N. (2016), "Direct tensile testing of self-compacting concrete", *Constr. Build. Mater.*, **112**, 903-906. https://doi.org/10.1016/j.conbuildmat.2016.02.215

Aliabadian, Z., Zhao, G.F. and Russell, A.R. (2019), "Failure, crack initiation and the tensile strength of transversely isotropic rock using the Brazilian test", *Int. J. Rock Mech. Mining Sci.*, **122**, 104073. https://doi.org/10.1016/j.ijrmms.2019.104073

ASTM D2936-08 (2008), Standard test method for splitting tensile strength of intact rock core specimens, Annual Book of ASTM Standards, Vol. 4, ASTM, West Conshohocken, PA, USA.

ASTM D3967-16 (2016), Standard Test Method for Splitting Tensile Strength of Intact Rock Core Specimens, Annual Book of ASTM Standards, Vol. 4, ASTM, West Conshohocken, PA, USA.

Bieniawski, Z.T. and Hawkes, I. (1978), "Suggested method for determining tensile strength of rock materials", *Int. J. Rock Mech. Mining Sci. & Geomechanics Abstracts*, **15**, 99-103. https://doi.org/10.1016/0148-9062(78)91677-7

Chen, W.F. and Trumbauer, B.E. (1972), "Double-punch test and tensile strength of concrete", *J. Mater. ASTM*, **7**(2), 148-154.

Crouch, S.L. (1976), "Analysis of stresses and displacements around underground excavations: an application of the displacement discontinuity method", University of Minnesota Geomechanics Report, Minneapolis, MN, USA.

Cundall, P.A. and Strack, O.D.L. (1979), "A discrete numerical model for granular assemblies", *Geotechnique*, **29**(1), 47-65. https://doi.org/10.1680/geot.1979.29.1.47

Denneman, E., Kearsley, E.P. and Visser, A.T. (2011), "Splitting tensile test for fibre re-inforced concrete", *Mater. Struct.*, **44**(8), 1441-1449. https://doi.org/10.1617/s11527-011-9709-x

Erarslan, N. and Williams, D.J. (2012), "Experimental, numerical and analytical studies on tensile strength of rocks", *Int. J. Rock Mech. Min. Sci.*, **49**, 21-30. https://doi.org/10.1016/j.ijrmms.2011.11.007

Forti, T.L., Forti, N., Santos, F.L. and Carnio, M.A. (2019), "The continuous-discontinuous Galerkin method applied to crack propagation", *Comput. Concrete, Int. J.*, **23**(4), 235-243. https://doi.org/10.12989/cac.2019.23.4.235

Ghaffar, A., Chaudhry, M.A. and Ali, M.K. (2005), "A new approach for measurement of tensile strength of concrete", *J. Res. Sci., Bahauddin Zakariya Univ.*, Multan, Pakistan, **16**(1), 1-9.

Gorski, B., Conlon, B. and Ljunggren, B. (2007), "Determination of the direct and indirect tensile strength on cores from borehole KFM01D", CANMET-MMSL, Mining and Mineral Sciences Laboratories, Natural Resources Canada, pp. 7-76.

Haeri, H., Khaloo, A. and Marji, M.F. (2015), "Fracture analyses of different pre-holed concrete specimens under compression", *Acta mechanica sinica*, **31**(6), 855-870. https://doi.org/10.1007/s10409-015-0436-3

Hannant, D.J. (1972), "The tensile strength of concrete: a review paper", *Struct. Eng.*, **50**(7), 253-257.

Hosseini_Nasab, H. and Fatehi Marji, M. (2007), "A semi-infinite higher-order displacement discontinuity method and its application to the quasistatic analysis of radial cracks produced by blasting", *J. Mech. Mater. Struct.*, **2**(3), 439-458.

Hu, S., Xu, A., Hu, X. and Yin, Y. (2016), "Study on fracture characteristics of reinforced concrete wedge splitting tests", *Comput. Concrete, Int. J.*, **18**(3), 337-354. https://doi.org/10.12989/cac.2016.18.3.337

Itasca Consulting Group Inc. (2003), PFC2D (particle flow code in 2dimensions) version 3.0, **41**(8), 1329-1364.

Khan, M.I. (2012), "Direct tensile strength measurement of concrete", *Appl. Mech. Mater.*, **117**, 9-14. https://doi.org/10.4028/www.scientific.net/AMM.117-119.9

Kim, J. and Taha, M.R. (2014), "Experimental and numerical evaluation of direct tension test for cylindrical concrete specimens", *Adv. Civ. Eng.*, 1-8. https://doi.org/10.1155/2014/156926

Li, S., Wang, H., Li, Y., Li, Q., Zhang, B. and Zhu, H. (2016), "A new mini-grating absolute displacement measuring system for static and dynamic geomechanical model tests", *Measurement*, **82**, 421-431. https://doi.org/10.1016/j.measurement.2017.04.002

Liao, Z.Y., Zhu, J.B. and Tang, C.A. (2019), "Numerical investigation of rock tensile strength determined by direct tension, Brazilian and three-point bending tests", *Int. J. Rock Mech. Mining Sci.*, **115**, 21-32. https://doi.org/10.1016/j.ijrmms.2019.01.007

Liu, Y.I., Dai, F., Xu, N., Zhao, T. and Feng, P. (2018), "Experimental and numerical investigation on the tensile fatigue properties of rocks using the cyclic flattened Brazilian disc method", *Soil Dyn. Earthq. Eng.*, **105**, 68-82. https://doi.org/10.1016/j.soildyn.2017.11.025

Marji, M.F. (1997), "Modelling of cracks in rock fragmentation with a higher order displacement discontinuity method", Ph.D. Thesis in Mining Engineering (Rock Mechanics), **1**(1), 167.

Marji, M.F. (2013), "On the use of power series solution method in the crack analysis of brittle materials by indirect boundary element method", *Eng. Fract. Mech.*, **98**, 365-382. https://doi.org/10.1016/j.engfracmech.2012.11.015

Marji, M.F., Hosseini-Nasab, H. and Kohsary, A.H. (2007), "A new cubic element formulation of the displacement discontinuity method using three special crack tip elements for crack analysis", *JP J. Solids Struct.*, **1**(1), 61-91.

Martin, C.D. (2014), "The direct and Brazilian tensile strength of rock in the light of size effect and bimodularity", *American Rock Mechanics Association, 48th U.S. Rock Mechanics/ Geomechanics Symposium*, June, Minneapolis, MN, USA.

Maruvanchery, V. and Kim, E. (2019), "Effects of water on rock fracture properties: Studies of mode I fracture toughness, crack propagation velocity, and consumed energy in calcite-cemented sandstone", *Geomech. Eng., Int. J.*, **17**(1), 57-67. https://doi.org/10.12989/gae.2019.17.1.057

Mosaberpanah, M.A. and Eren, O. (2016), "Statistical flexural toughness modeling of ultra-high performance concrete using response surface method", *Comput. Concrete, Int. J.*, **17**(4), 33-39. https://doi.org/10.12989/cac.2016.17.4.477

Omar, H., Ahmad, J., Nahazanan, H., Mohammed, T.A. and Yusoff, Z.M. (2018), "Measurement and simulation of diametrical and axial indirect tensile tests for weak rocks", *Measurement*, **127**, 299-307. https://doi.org/10.1016/j.measurement.2018.05.067

Pan, B., Gao, Y. and Zhong, Y. (2014), "Theoretical analysis of overlay resisting crack propagation in old cement concrete pavement", *Struct. Eng. Mech., Int. J.*, **52**(4), 167-181. https://doi.org/10.1007/978-94-007-4566-7_51

Potyondy, D.O. and Cundall, P.A. (2004), "A bonded-particle model for rock", *Int. J. Rock Mech. Min. Sci.*, **41**(8), 1329-1364.

Ramadoss, P. and Nagamani, K. (2013), "Stress-strain behavior and toughness of high-performance steel fiber reinforced

concrete in compression", *Comput. Concrete*, *Int. J.*, **11**(2), 55-65. https://doi.org/10.12989/cac.2013.11.2.149
Sanford, R.J. (2003), *Principles of Fracture Mechanics*, Pearson Education, hIC., Upper Saddle River, NJ, USA, pp. 1-15.
Sardemir, M. (2016), "Empirical modeling of flexural and splitting tensile strengths of concrete containing fly ash by GEP", *Comput. Concrete*, *Int. J.*, **17**(4), 489-498. https://doi.org/10.12989/cac.2016.17.4.489
Sarfarazi, V., Faridi, H.R., Haeri, H. and Schubert, W. (2015), "A new approach for measurement of anisotropic tensile strength of concrete", *Adv. Concrete Constr.*, *Int. J.*, **3**(4), 269-282. https://doi.org/10.12989/acc.2015.3.4.269
Sarfarazi, V., Haeri, H. and Shemirani, A.B. (2017), "Direct and indirect methods for determination of mode I fracture toughness using PFC2D", *Comput. Concrete*, *Int. J.*, **20**(1), 1-10. https://doi.org/10.12989/cac.2017.20.1.039
Shang, J., Duan, K., Gui, Y., Handley, K. and Zhao, Z. (2018), "Numerical investigation of the direct tensile behaviour of laminated and transversely isotropic rocks containing incipient bedding planes with different strengths", *Comput. Geotech.*, **104**, 373-388. https://doi.org/10.1016/j.compgeo.2017.11.007
Shou, K.J. and Crouch, S.L. (1995), "A higher order displacement discontinuity method for analysis of crack problems", *Int. J. Rock Mech. Min. Sci. Geomech. Abstract*, **32**, 49-55.
Shuraim, A.B., Aslam, F., Hussain, R.R. and Alhozaimy, A.M. (2016), "Analysis of punching shear in high strength RC panels-experiments, comparison with codes and FEM results", *Comput. Concrete*, *Int. J.*, **17**(6), 739-760. https://doi.org/10.12989/cac.2016.17.6.739
Silva, R.V., De Brito, J. and Dhir, R.K. (2015), "Tensile strength behaviour of recycled aggregate concrete", *Constr. Build. Mater.*, **83**, 108-118. https://doi.org/10.1016/j.conbuildmat.2015.03.034
Sun, W., Du, H., Zhou, F. and Shao, J. (2019), "Experimental study of crack propagation of rock-like specimens containing conjugate fractures", *Geomech. Eng.*, *Int. J.*, **17**(4), 323-331. https://doi.org/10.12989/gae.2019.17.4.323
Swaddiwudhipong, S., Lu, H.R. and Wee, T.H. (2003), "Direct tension test and tensile strain capacity of concrete at early age", *Cem. Concr. Res.*, **33**, 2077-2084. https://doi.org/10.1016/S0008-8846(03)00231-X
Tran, K.Q., Satomi, T. and Takahashi, H. (2019), "Tensile behaviors of natural fiber and cement reinforced soil subjected to direct tensile test", *J. Build. Eng.*, **24**, 100748. https://doi.org/10.1016/j.jobe.2019.100748
Wang, Q.Z., Jia, X.M., Kou, S.Q., Zhang, Z.X. and Lindqvist, P.A. (2004), "The flattened Brazilian disc specimen used for testing elastic modulus, tensile strength and fracture toughness of brittle rocks: analytical and numerical results", *Int. J. Rock Mech. Min. Sci.*, **41**, 245-253. https://doi.org/10.1016/S1365-1609(03)00093-5
Wei, X.X. and Chau, K.T. (2013), "Three dimensional analytical solution for finite circular cylinders subjected to indirect tensile test", *Int. J. Solids Struct.*, **50**, 2395-2406. https://doi.org/10.1016/j.ijsolstr.2013.03.026
Whittaker, B.N., Singh, R.N. and Sun, G. (1992), "Rock fracture mechanics. Principles, design and applications", Developments in Geotechnical Engineering, 71. Elsevier, Amsterdam, Netherlands.
Xie, N.X. and Liu, W.Y. (1989), "Determining tensile properties of mass concrete by direct tensile test", *ACI Mater. J.*, **86**(3), 214-219.
Yaylaci, M. (2016), "The investigation crack problem through numerical analysis", *Struct. Eng. Mech.*, *Int. J.*, **57**(6), https://doi.org/10.12989/sem.2016.57.6.1143
Zain, M.F.M., Mahmud, H.B., Ilham, A. and Faizal, M. (2002), "Prediction of splitting tensile strength of high-performance concrete", *Cem. Concr. Res.*, **32**, 1251-1257. https://doi.org/10.1016/S0008-8846(02)00768-8
Zhang, Z.X. (2002), "An empirical relation between mode I fracture toughness and the tensile strength of rock", *Int. J. Rock Mech. Mining Sci. & Geomech. Abstracts*, **93**, 401-406.
Zhang, D., Hou, S., Bian, J. and He, L. (2016), "Investigation of the micro-cracking behavior of asphalt mixtures in the indirect tensile test", *Eng. Fract. Mech.*, **163**, 416-425. https://doi.org/10.1016/j.engfracmech.2016.05.020
Zheng, W., Kwan, A.K.H. and Lee, P.K.K. (2001), "Direct tension test of concrete", *ACI Mater. J.*, **98**(1), 63-71.
Zhou, F.P. (1988), "Some aspects of tensile fracture behaviour and structural response of cementitious materials", Report TVBM-1008, Division of Building Materials, Lund Institute of Technology.

CC